Recent Results from PHOBOS at RHIC

Robert Pak for the PHOBOS Collaboration

B.B.Back[1], M.D.Baker[2], D.S.Barton[2], R.R.Betts[6], M.Ballintijn[4], A.A.Bickley[7], R.Bindel[7], A.Budzanowski[3], W.Busza[4], A.Carroll[2], M.P.Decowski[4], E.García[6], N.George[1,2], K.Gulbrandsen[4], S.Gushue[2], C.Halliwell[6], J.Hamblen[8], G.A.Heintzelman[2], C.Henderson[4], D.J.Hofman[6], R.S.Hollis[6], R.Hołyński[3], B.Holzman[2], A.Iordanova[6], E.Johnson[8], J.L.Kane[4], J.Katzy[4,6], N.Khan[8], W.Kucewicz[6], P.Kulinich[4], C.M.Kuo[5], W.T.Lin[5], S.Manly[8], D.McLeod[6], J.Michałowski[3], A.C.Mignerey[7], R.Nouicer[6], A.Olszewski[3], R.Pak[2], I.C.Park[8], H.Pernegger[4], C.Reed[4], L.P.Remsberg[2], M.Reuter[6], C.Roland[4], G.Roland[4], L.Rosenberg[4], J.Sagerer[6], P.Sarin[4], P.Sawicki[3], W.Skulski[8], S.G.Steadman[4], P.Steinberg[2], G.S.F.Stephans[4], M.Stodulski[3], A.Sukhanov[2], J.-L.Tang[5], R.Teng[8], A.Trzupek[3], C.Vale[4], G.J.van Nieuwenhuizen[4], R.Verdier[4], B.Wadsworth[4], F.L.H.Wolfs[8], B.Wosiek[3], K.Woźniak[3], A.H.Wuosmaa[1], B.Wysłouch[4]

[1] Argonne National Laboratory, [2] Brookhaven National Laboratory, [3] Institute of Nuclear Physics, Kraków, Poland, [4] Massachusetts Institute of Technology, [5] National Central University, Chung-Li, Taiwan, [6] University of Illinois at Chicago, [7] University of Maryland, [8] University of Rochester

The PHOBOS experiment at RHIC has recorded measurements for Au-Au collisions spanning nucleon-nucleon center-of-mass energies from $\sqrt{s_{NN}} = 19.6$ GeV to 200 GeV. Global observables such as elliptic flow and charged particle multiplicity provide important constraints on model predictions that characterize the state of matter produced in these collisions. The nearly 4π acceptance of the PHOBOS experiment provides excellent coverage for complete flow and multiplicity measurements. Results including beam energy and centrality dependencies are presented and compared to elementary systems.

1. Introduction

The results presented here are based on PHOBOS data taken during the first two RHIC physics runs for Au-Au collisions at $\sqrt{s_{NN}} = 19.6$, 130 and 200 GeV. Event centrality (impact parameter) is characterized by the number of participating nucleons, N_{part}, allowing direct comparison to elementary systems, like pp, $\overline{p}p$ and $e^+e^- \rightarrow$ hadrons. The PHOBOS detector consists mainly of silicon pad sensors to perform particle tracking, vertex detection and multiplicity measurements. This set of detectors has nearly full azimuthal coverage over a large pseudorapidity range $|\eta| < 5.4$. Details of the layout of the Si sensors can be found elsewhere [1,2]. Our methods for event triggering and centrality selection have been previously described [3,4]. The raw data came in the form of energy depositions from the passage of charged particles above threshold through individual Si pads, known as hits. The position of the primary collision vertex was determined on an event-by-event basis by extrapolating tracks found in the spectrometer arms and/or the vertex detector.

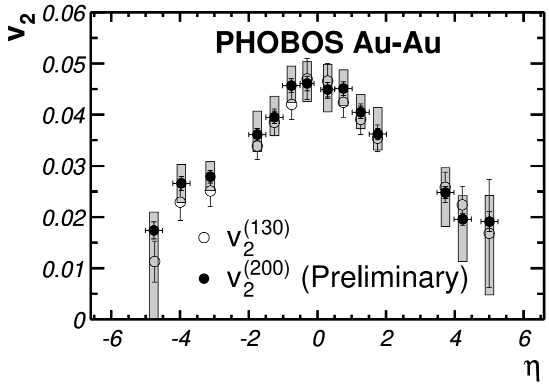

Figure 1. Elliptic flow as a function of pseudorapidity for Au-Au collisions at $\sqrt{s_{NN}} =$ 130 and 200 GeV. Error bars are statistical, and boxes represent 90% confidence level systematic errors on the 200 GeV data.

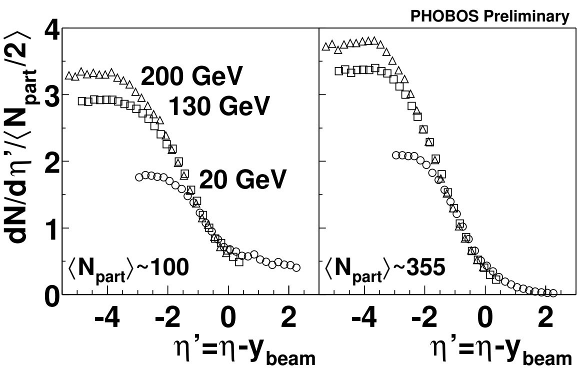

Figure 2. Charged particle pseudorapidity distributions scaled by the number of participant pairs for central (non-central) Au-Au collisions at $\sqrt{s_{NN}} = 19.6$, 130 and 200 GeV are shown in the right (left) panel. Systematic errors are not shown.

2. Flow

The particle emission pattern created in heavy-ion collisions can be probed by measuring azimuthal anisotropy about the event plane, *i.e.*, elliptic flow. The event plane was determined by a standard subevent technique [5] using hits in symmetric and uniform regions of the octagonal barrel multiplicity detector. The second Fourier coefficient of the hit azimuthal angle distribution, v_2, (elliptic flow) was evaluated by correlating the event plane to hits in a different region of the multiplicity detectors and corrected for event plane resolution. Details of this flow analysis are provided in Ref. [6].

Flow results are shown in Fig. 1, where the error bars indicate 1σ statistical errors. The 90% confidence level systematic errors are shown as boxes for the 200 GeV data points. The flow signal changes little with the increase in the center-of-mass energy of the collision from 130 to 200 GeV. Fig. 1 shows a substantial drop in v_2 as a function of $|\eta|$ in contradiction with the idea of longitudinal boost invariance over a broad rapidity range in RHIC collisions.

3. Multiplicity

Fig. 2 shows charged particle pseudorapidity distributions scaled by the number of participant pairs, $dN_{ch}/d\eta'/\langle N_{part}/2\rangle$ (where $\eta' = \eta - y_{\mathrm{beam}}$), measured at three different RHIC energies for peripheral ($\langle N_{part}\rangle \sim 100$) and central events ($\langle N_{part}\rangle \sim 355$), in the left and right panels, respectively. Shifting into the rest frame of one of the colliding nuclei clearly demonstrates the "limiting behavior" in the fragmentation region, *i.e.*, the distributions are independent of beam energy over a substantial range in η' [4]. Similar behavior has been observed in $\overline{p}p$ [7], pA [8], and e^+e^- [9] collisions over a large range

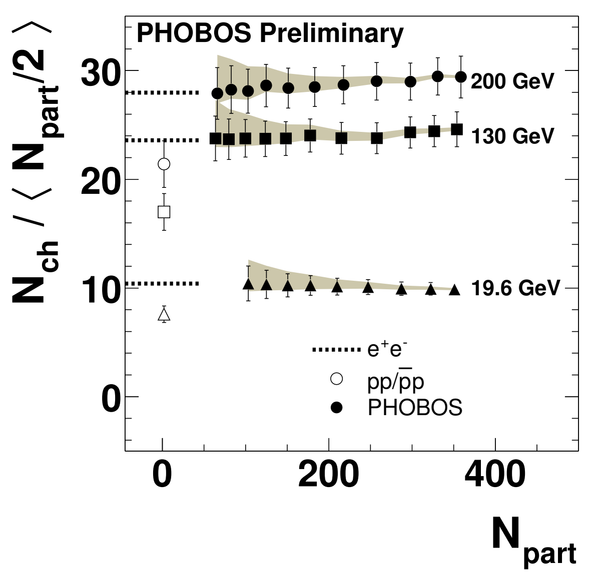

Figure 3. Centrality dependence of the total charged particle multiplicity per participant pair in Au-Au collisions at $\sqrt{s_{NN}}$ = 19.6, 130 and 200 GeV. Error bars include systematic error. The shaded band shows the uncertainty from high-η extrapolation. Also shown are results for e^+e^- and $\overline{p}p$ data.

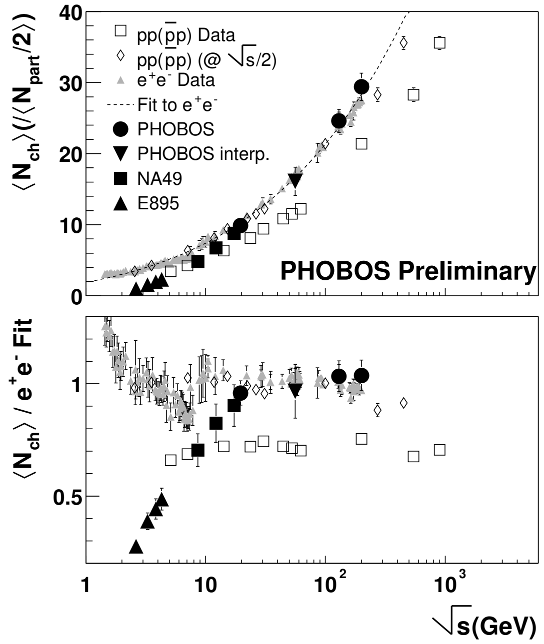

Figure 4. Comparison of the total charged particle multiplicity for elementary and heavy-ion collisions as a function of collision energy, as described in the text. In the bottom panel the data are divided by the e^+e^- fit shown in the top panel.

of energies. In Fig. 2 the extent of the limiting fragmentation region significantly grows with collision energy in sharp contrast to a boost-invariant scenario.

Comparison of the data at a fixed beam energy between the left and right panels of Fig. 2 demonstrates that even though the shapes of the distributions dramatically change, the extent of the fragmentation region is nearly independent of centrality. The total charged particle multiplicity, N_{ch}, was determined by integrating $dN_{ch}/d\eta'$, where the low energy data along with fits to the higher energy data was used to extrapolate out to larger η' for the higher energies. Repeating this procedure at each beam energy for all centrality classes results in Fig. 3, which shows $\langle N_{ch} \rangle / \langle N_{part}/2 \rangle$ is centrality independent.

In Fig. 4, $\langle N_{ch} \rangle / \langle N_{part}/2 \rangle$ in central heavy-ion collisions [10] is compared to e^+e^- and $pp/\overline{p}p$ data over a large range in collision energy, $\sqrt{s}$ [11]. $\langle N_{ch} \rangle / \langle N_{part}/2 \rangle$ is observed to lie below pp at low energies, passing through the pp data around $\sqrt{s} \sim 10$ GeV, and then gradually converging with the e^+e^- trend above CERN SPS energies. These comparisons can be made clearer by dividing all of the data with a fit to the e^+e^- data [12] as shown in the lower panel of Fig. 4. The $pp/\overline{p}p$ data (open squares) follows the same trend as e^+e^-, but agrees better if rescaled to an "effective energy" $\sqrt{s}_{\text{eff}} = \sqrt{s}/2$ (open diamonds), which approximately accounts for the leading particle effect seen in pp collisions [13]. Ref. [13] finds that bulk particle production in pp and e^+e^- data does not depend in detail on the collision system, but rather the energy available for particle production. In this scenario, the Au-Au data suggests a substantially reduced leading particle effect in central collisions of heavy nuclei at high energy [14].

Modulation of the leading particle effect in nuclear collisions may be the result of multiple scattering. For example, each participating nucleon is typically struck three times on average as it passes through the oncoming Au nucleus for $N_{part} > 65$. This rescattering could transfer much more of the initial longitudinal energy into particle production. This naturally leads to the scaling of total particle production in heavy-ion collisions with N_{part}, as seen in Fig. 3, suggestive of the "wounded nucleon model" [15] but with the scaling factor determined by e^+e^- rather than pp [14].

4. Summary

Recent results from PHOBOS at RHIC indicate clear evidence of limiting fragmentation in Au-Au collisions. Also, longitudinal boost invariance occurs only over a limited region, because this fragmentation region grows with beam energy, along with the pronounced drop in flow at high η. Finally, there is a striking similarity of particle production in e^+e^- and particle production per participating nucleon pair in Au-Au collisions.

Acknowledgments: This work was partially supported by US DoE grants DE-AC02-98CH10886, DE-FG02-93ER40802, DE-FC02-94ER40818, DE-FG02-94ER40865, DE-FG02-99ER41099, W-31-109-ENG-38, and NSF grants 9603486, 9722606 and 0072204. The Polish group was partially supported by KBN grant 2-P03B-10323. The NCU group was partially supported by NSC of Taiwan under contract NSC 89-2112-M-008-024.

REFERENCES

1. H. Pernegger *et al.*, Nucl. Inst. Meth. **A473** (2001) 197.
2. B. B. Back *et al.*, Nucl. Phys **A698** (2002) 416c.
3. B. B. Back *et al.*, Phys. Rev. C **65** (2002) 061901R.
4. B. B. Back *et al.*, arXiv:nucl-ex/0210015, submitted to Phys. Rev. Lett.
5. A. M. Poskanzer and S. A. Voloshin, Phys. Rev. C **58** (1998) 1671.
6. B. B. Back *et al.*, Phys. Rev. Lett. **89** (2002) 222301.
7. G. J. Alner *et al.*, Z. Phys. C **33** (1986) 1.
8. J. E. Elias *et al.*, Phys. Rev. D **22** (1980) 13.
9. P. Abreu *et al.*, Phys. Lett. B **459** (1999) 397.
10. J. Klay, U.C. Davis PhD. Thesis (2001), S. V. Afanasiev *et al.*, arXiv:nucl-ex/0205002.
11. D. E. Groom *et al.*, Eur. Phys. J. C **15** (2000) 1.
12. A. H. Mueller, Nucl. Phys. B **213** (1983) 85.
13. M. Basile *et al.*, Phys. Lett. B **92** (1980) 367; Phys. Lett. B **95** (1980) 311.
14. P. Steinberg *et al.*, arXiv:nucl-ex/0210024.
15. J. E. Elias *et al.* Phys. Rev. Lett. **41** (1978) 285, A. Białas, B. Bleszyński and W. Czyż, Nucl. Phys. **B111** (1976) 461.